

Supplemental Material for

Fast, Accurate and Reliable Protocols for Routine  
Calculations of Protein-Ligand Binding Affinities in  
Drug-Design Projects Using AMBER GPU-TI with  
ff14SB/GAFF.

*Xibing He<sup>†</sup>, Shuhan Liu,<sup>†</sup> Tai-Sung Lee,<sup>‡</sup> Beihong Ji,<sup>†</sup> Viet H. Man,<sup>†</sup> Darrin M. York,<sup>‡</sup> and  
Junmei Wang<sup>†,\*</sup>*

<sup>†</sup> Department of Pharmaceutical Sciences and Computational Chemical Genomics Screening  
Center, School of Pharmacy, University of Pittsburgh, Pittsburgh, Pennsylvania 15261, United  
States

<sup>‡</sup> Laboratory for Biomolecular Simulation Research, Center for Integrative Proteomics Research  
and Department of Chemistry and Chemical Biology, Rutgers University, Piscataway, New  
Jersey 08854, United States

\* Corresponding author: Junmei Wang, [junmei.wang@pitt.edu](mailto:junmei.wang@pitt.edu)

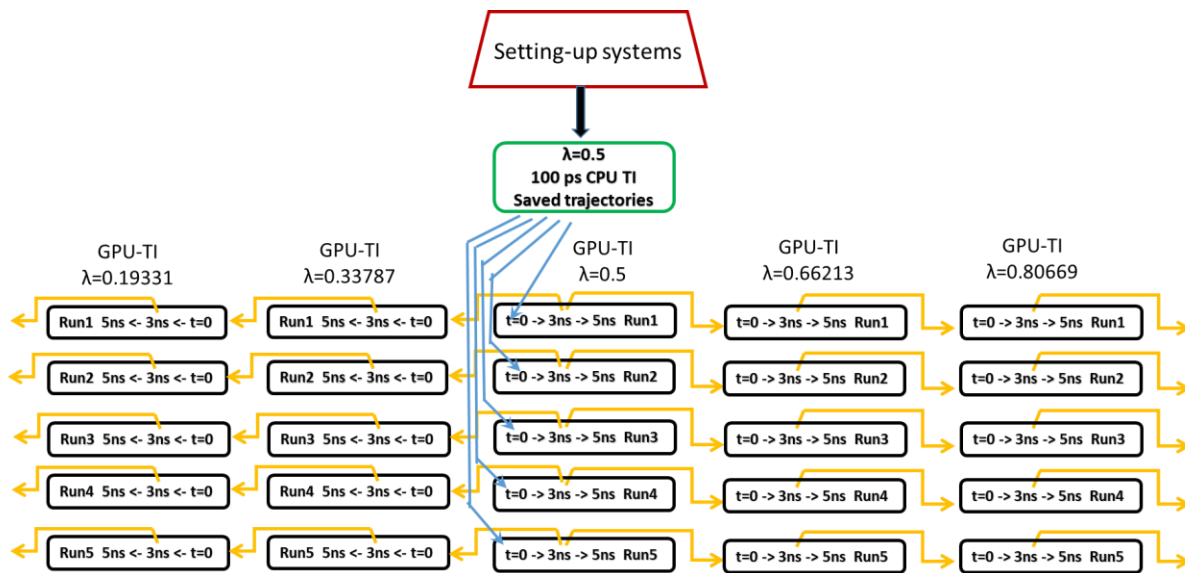


Figure S1. The schedule of initial equilibration and later  $\lambda$  expanding.

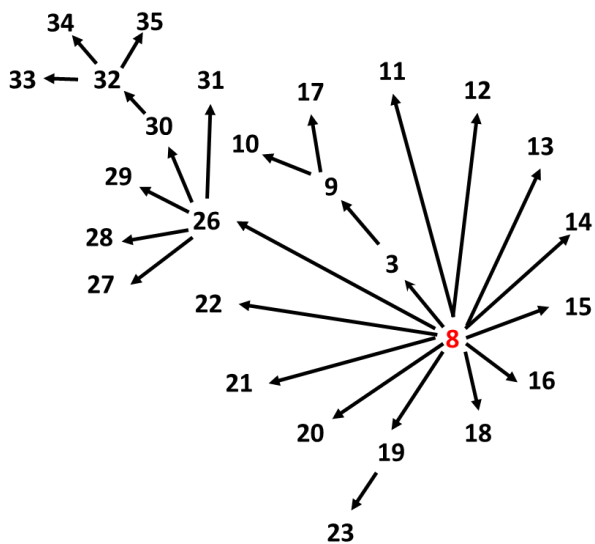


Figure S2. The alchemical transformation paths of PTP1B ligands adopted in the TI calculations. The detailed structure of each ligand is presented in Ref S1. All ligands listed in Tables 1-3 in Ref S1 were set for calculations, plus the Ligand 3 in Figure 1 of Ref S1 as an intermediate compound between Ligand 8 and Ligands 9, 10 & 17. Among these ligands, 3, 9, 26 & 29 were omitted by the Schrodinger FEP+ study (Ref S2). The ligand 8 was used as the common reference compound and its experimental  $\Delta G$  value was adopted to derive the calculated  $\Delta G$  values of all other ligands. See the supplementary Excel file.

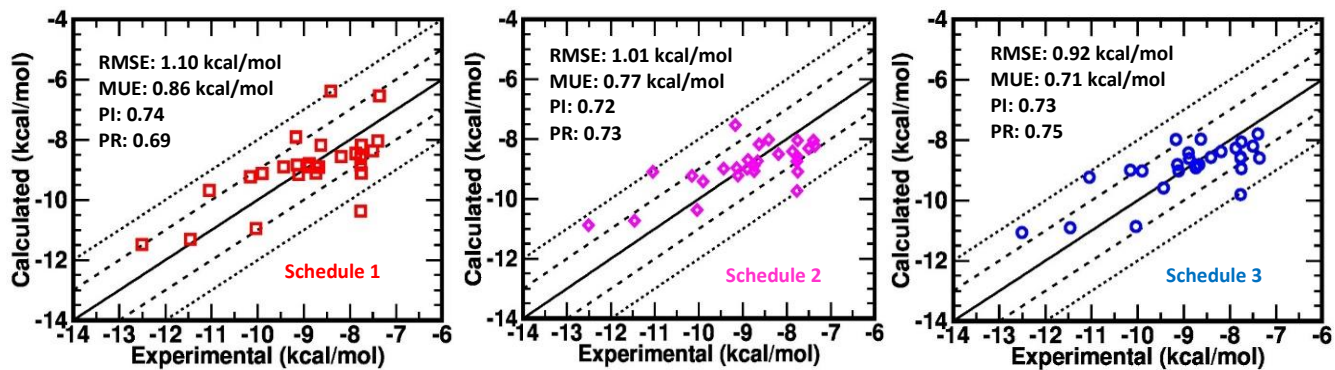


Figure S3. The performance of AMBER GPU-TI on the PTP1B system with 3 different  $\lambda$  schedules and corresponding methods of integration of  $\partial U/\partial\lambda$ .

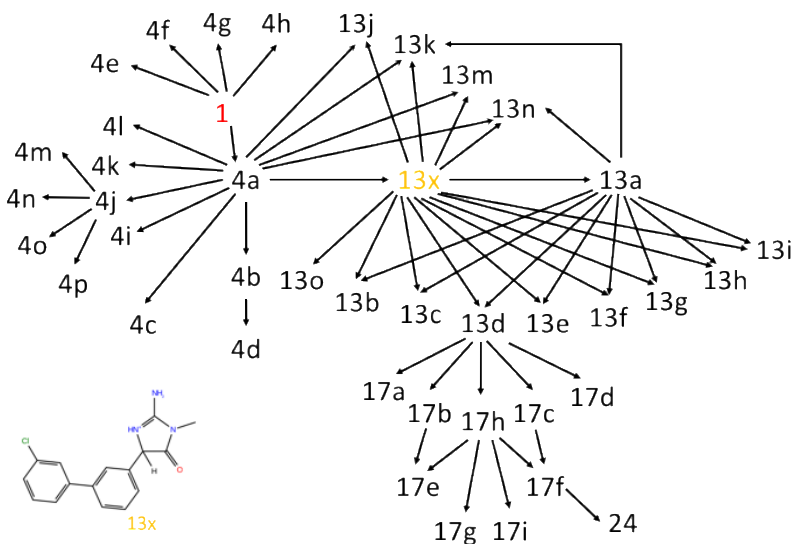


Figure S4. The alchemical transformation paths for the BACE system. The detailed structure of each ligand is presented in Ref S3 except for Ligand 13x, which is a pseudo intermediate compound and whose structure is shown at the left bottom corner. All ligands listed in Tables 1, 3, 4 & 5 in Ref S3 were set for calculations (note: Ligand 19 in Table 5 is the R-enantiomer of Ligand 17h in Table 4), plus the Ligand 1 in Figure 1 of Ref S3. Among these ligands, 1, 4e, 4f, 4g & 4h were omitted by the Schrodinger FEP+ study (Ref S2). The ligand 1 was used as the common reference compound and its experimental  $\Delta G$  value was adopted to derive the calculated  $\Delta G$  values of all other ligands. For this BACE system, we exploited the effects of different paths to the same query ligands and the reported  $\Delta G$  for these ligands were the arithmetic averages of different mutation paths. Note that they are NOT for closed-cycles analysis. See the supplementary Excel file.

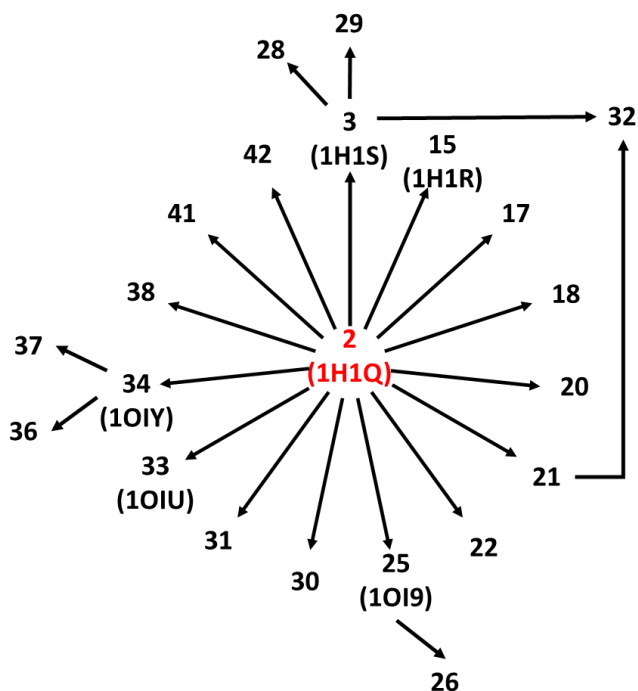


Figure S5. The alchemical transformation paths for the CDK2 system. The detailed structure of each ligand is presented in Ref S4. All ligands listed in Tables 2 in Ref S4 with specific IC50 values (in the unit of  $\mu\text{M}$  or nM, not a percentage value at 10  $\mu\text{M}$ ) were set for calculations except for Ligand 39, which has a charged  $-\text{COO}^-$  group but other ligands are neutral. Among these ligands, 18, 36, 37, 38, 41 & 42 were omitted by the Schrodinger FEP+ study (Ref S2). The Ligand 2 was used as the common reference compound and its experimental  $\Delta\text{G}$  value was adopted to derive the calculated  $\Delta\text{G}$  values of all other ligands. We tested two mutation paths for Ligand 32 and the calculated  $\Delta\text{G}$  values for Ligand 32 from these two paths are close (with a difference of 0.35 kcal/mol), and the average was reported as the final  $\Delta\text{G}$  value for Ligand 32. See the supplementary Excel file.

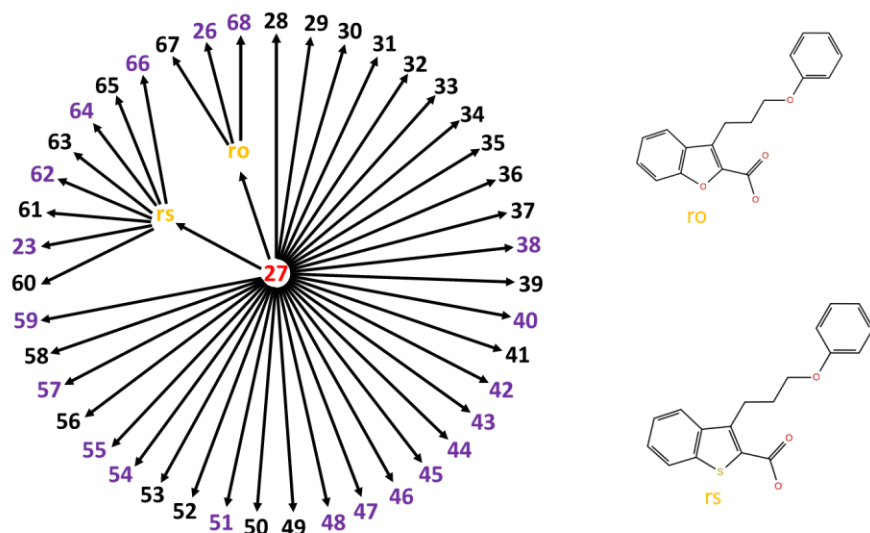


Figure S6. The alchemical transformation paths for the MCL1 system. The detailed structure of each ligand is presented in Ref S5 except for ro and rs, which are created intermediate molecules and whose structures are shown on the right side. All ligands listed in Tables 3 in Ref S5 were set for calculations. Among these ligands, 55 & 59 were omitted by the Schrodinger FEP+ study (Ref S2). The Ligand 27 was used as the common reference compound and its experimental  $\Delta G$  value was adopted to derive the calculated  $\Delta G$  values of all other ligands. The ligands shown in brown color have bicyclic aromatic rings or heterocycles which are hard to flip automatically during a shot MD simulation. Therefore, two separate conformations of these ligands (with the bicyclic rings flipped or not) are adopted to set up the mutation simulations in complexes, and the corrected free energies were calculated as described in our supplementary Excel file and in Ref S6.

Table S1. The effects of changing water models and sizes of simulation boxes on 7 mutation pairs in the PTP1B system.

Mutation pair	Calculation errors for $\Delta\Delta G$ (kcal/mol)		
	TIP3P water model & 12 Å water shell for complexes and 12 Å water shell for solutions	SPC/E water model & 12 Å water shell for complexes and 12 Å water shell for solutions	TIP3P water model & 5 Å water shell for complexes and 10 Å water shell for solutions
3 → 8	0.31	0.13	0.28
8 → 11	-0.39	-1.23	-0.42
8 → 12	0.07	1.22	0.54
8 → 13	-0.79	-1.57	-1.15
8 → 14	-0.43	0.18	-0.88
8 → 15	0.26	-0.84	-0.98
8 → 16	1.06	1.23	0.87
$\Delta\Delta G$ MUE	0.47	0.91	0.73
$\Delta\Delta G$ RMSE	0.57	1.05	0.79

Table S2. The number of atoms, the size of simulation boxes, and the averaged wall time per ns TI simulation with one Nvidia GTX1080 GPU card for each protein system.

	BACE		CDK2		MCL1		PTP1B	
	Complex	Solution	Complex	Solution	Complex	Solution	Complex	Solution
Atoms	53800	3960	45600	4270	30590	3970	48240	4070
Box size (Å <sup>3</sup> )	88*75*97	44*34*39	68*81*99	41*38*40	76*68*72	40*35*40	96*82*73	36*40*37
Wall time / ns (hrs)	0.71	0.16	0.60	0.17	0.50	0.16	0.65	0.17

## REFERENCES:

(S1) Wilson, D. P.; Wan, Z. K.; Xu, W. X.; Kirincich, S. J.; Follows, B. C.; Joseph-McCarthy, D.; Foreman, K.; Moretto, A.; Wu, J.; Zhu, M.; Binnun, E.; Zhang, Y. L.; Tam, M.; Erbe, D. V.; Tobin, J.; Xu, X.; Leung, L.; Shilling, A.; Tam, S. Y.; Mansour, T. S.; Lee, J., Structure-based optimization of protein tyrosine phosphatase 1B inhibitors: From the active site to the second phosphotyrosine binding site. *J. Med. Chem.* **2007**, 50 (19), 4681-4698.

(S2) Wang, L.; Wu, Y. J.; Deng, Y. Q.; Kim, B.; Pierce, L.; Krilov, G.; Lupyán, D.; Robinson, S.; Dahlgren, M. K.; Greenwood, J.; Romero, D. L.; Masse, C.; Knight, J. L.; Steinbrecher, T.; Beuming, T.; Damm, W.; Harder, E.; Sherman, W.; Brewer, M.; Wester, R.; Murcko, M.; Frye, L.; Farid, R.; Lin, T.; Mobley, D. L.; Jorgensen, W. L.; Berne, B. J.; Friesner, R. A.; Abel, R. Accurate and Reliable Prediction of Relative Ligand Binding Potency in Prospective Drug Discovery by Way of a Modern Free-Energy Calculation Protocol and Force Field. *J. Am. Chem. Soc.* 2015, 137, 2695-2703.

(S3) Cumming, J. N.; Smith, E. M.; Wang, L.; Misiaszek, J.; Durkin, J.; Pan, J.; Iserloh, U.; Wu, Y.; Zhu, Z.; Strickland, C.; Voigt, J.; Chen, X.; Kennedy, M. E.; Kuvelkar, R.; Hyde, L. A.; Cox, K.; Favreau, L.; Czarniecki, M. F.; Greenlee, W. J.; McKittrick, B. A.; Parker, E. M.; Stamford, A. W., Structure based design of iminohydantoin BACE1 inhibitors: identification of an orally available, centrally active BACE1 inhibitor. *Bioorg. Med. Chem. Lett.* **2012**, 22 (7), 2444-2449.

(S4) Hardcastle, I. R.; Arris, C. E.; Bentley, J.; Boyle, F. T.; Chen, Y.; Curtin, N. J.; Endicott, J. A.; Gibson, A. E.; Golding, B. T.; Griffin, R. J.; Jewsbury, P.; Menyerol, J.; Mesguiche, V.; Newell, D. R.; Noble, M. E.; Pratt, D. J.; Wang, L. Z.; Whitfield, H. J., N2-substituted O6-cyclohexylmethylguanidine derivatives: potent inhibitors of cyclin-dependent kinases 1 and 2. *J. Med. Chem.* **2004**, 47 (15), 3710-3722.

(S5) Friberg, A.; Vigil, D.; Zhao, B.; Daniels, R. N.; Burke, J. P.; Garcia-Barrantes, P. M.; Camper, D.; Chauder, B. A.; Lee, T.; Olejniczak, E. T.; Fesik, S. W., Discovery of Potent Myeloid Cell Leukemia 1 (Mcl-1) Inhibitors Using Fragment-Based Methods and Structure-Based Design. *J. Med. Chem.* **2013**, 56 (1), 15-30.

(S6) Kaus, J.W.; Harder, E.; Lin, T.; Abel, R.; McCammon, J. A.; Wang, L. How to deal with multiple binding poses in alchemical relative protein-ligand binding free energy calculations. *J. Chem. Theory Comput.* **2015**, 11, 2670-2679.